Vibratory Pile Driving and Deep Soil Compaction - TRANSVIB2002,
Holeyman, VandenBerghe & Charue (eds.), © 2002 Swets & Zeitlinger, Lisse, ISBN 90 5809 521 5

Soil Behavior under Vibratory Driving

Alain E. Holeyman
Université Catholique de Louvain, Louvain-la-Neuve, Belgium

ABSTRACT : Vibratory driving of piles and soil densification raise several engineering issues including the long-term bearing capacity of the installed pile, its vibratory penetration resistance, the performance of vibrators, the degradation and liquefaction of the soil around the vibrated profile, and vibratory nuisance to the environment. An argument is made that those issues will be adequately tackled once combined into a comprehensive framework of analysis where proper understanding of soil behavior is the key. The present paper reviews our current engineering ability to assess vibro-drivability, i.e. predicting the vibratory penetration log of a given pile into a given soil profile using a given vibrator. Testing undertaken to provide insight into the pile-soil-vibrator interaction and its modelling is then emphasized. Several available methods to establish the vibratory performance of a pile from its vibratory capacity are discussed. A rational procedure to model the dynamic nonlinear soil structure interaction during pile vibratory driving is discussed in more detail. Degradation of the skin friction upon cyclic shear stress is evaluated by applying elements of earthquake engineering practice used to assess liquefaction potential. The present ability to assess the vibratory capacity of a pile from the monitoring of its vibratory performance is critically reviewed. Finally, suggestions for further research, design and practice are provided.

1 INTRODUCTION

1.1 *Scope*

The main purpose of this key-note paper is to present the author's present view on soil engineering issues relating to the drivability of piles and sheet-piles using vibrators and the inverse problem, i.e. deriving the pile resistance from its vibratory performance. It is based on a survey of the relevant literature and original research in the area.

1.2 *Historical Development*

The vibratory driving technique appears to date back to the early 30's when it was simultaneously developed in the former USSR and in Germany (Rodger and Littlejohn, 1980). The observation by the Russian soil dynamics researcher Pavyluk that soil resistance could be reduced thanks to vibrations led to the industrial use of vibrators to drive piles, according to Barkan, 1960. Extensive research on the effects of vibration on soils was conducted in the 40's and 50's by Barkan, while the vibratory driving technique was gaining acceptance as an economical and effective means of installing piles and sheet piles in appropriate soil conditions. Major vibrators manufacturers are now located in Germany, France, The Netherlands, USA, the Former Soviet Union and Japan. Although technological developments have been brought to enhance the initial concept and extend commercial application of vibrators, little is mastered by the engineer when it comes to addressing soil related issues. That limitation in the engineering knowledge is viewed by many as an impediment for the vibratory driving technique to enjoy its full potential.

1.3 *Phenomena at Play*

Three major actors play a role in the mechanics of the vibratory driving process, as illustrated in Fig. 1 : (1) the pile to be driven, (2) the selected vibrator, and (3) the imposed soil conditions. The pile can be fully described by its material and geometry. The vibrator mechanical behavior can be assessed based on its specifications and operational range, as discussed in Section 2. Soil conditions are usually characterized by means of standard investigation tools such as CPT soundings, borings and laboratory tests.

Those investigation tools are geared towards answering general design questions (mostly static) but are not well suited to characterize soil behavior under pile installation conditions, specially if the piles are vibratory driven.

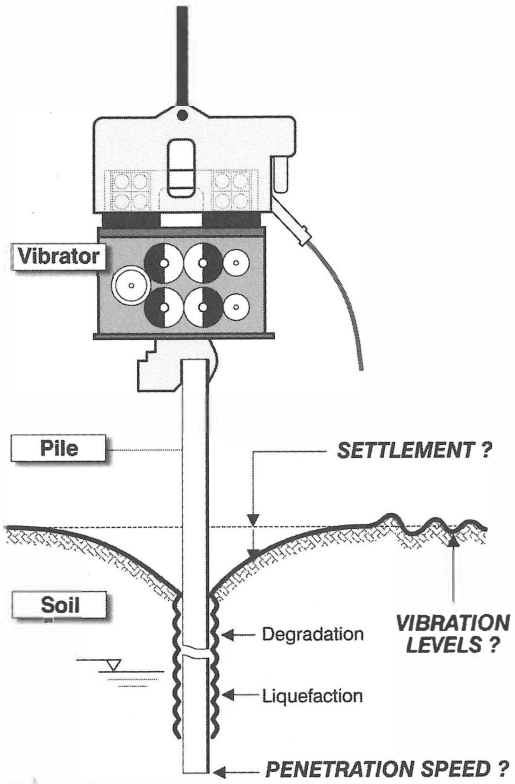

Figure 1. Vibratory Driving : Players and Issues

Because it is has been established for more than half a century that soil resistance during vibratory driving (likewise during impact driving) is lower than the long-term bearing capacity, these two resistances should be distinguished. As shown in Fig. 2, one can estimate the vibratory capacity from the long-term bearing capacity by taking soil degradation effects into account. Conversely, one can estimate the long-term bearing capacity from the vibratory capacity if soil set-up can be accounted for.

A fundamental understanding of soil behavior under vibratory loading is required to establish the relationship between the pile vibratory resistance and its long-term bearing capacity. Soil resistance degrades upon cyclic shearing mainly because of fatigue of the soil skeleton in cohesive soils (Vucetic, 1992), and of effective stress reduction in granular soils (Casagrande, 1938). The effective stress can be ultimately reduced to nearly zero, at which point the soil behaves in a fluid-like manner. These phenomena will be reviewed in more detail in Section 3.

1.4 *Engineering issues*

Engineering issues related to vibratory driving cover many facets, as illustrated in Figs. 1 and 2. They prompt the following questions :

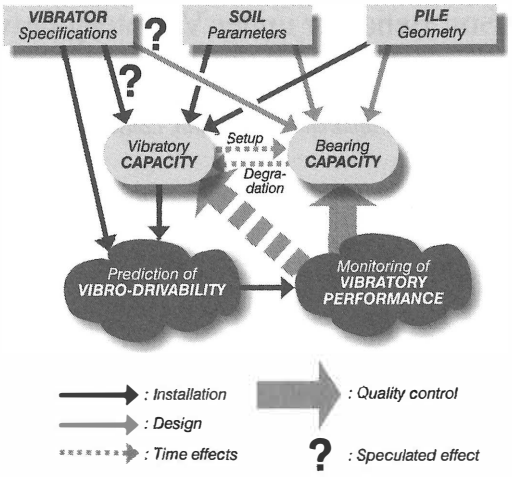

Figure 2. Installation and design process of vibratory driven piles

- What is the long-term bearing capacity of the installed pile? We know it depends on the pile geometry, on the soil parameters, but also on the vibratory process.
- How are the soil's long-term strength parameters influenced by the vibratory process? By how much will the soil compact, and what is the magnitude of the potentially induced settlement?
- How are vibrations transmitted to the surrounding soil, and how much potential damage can they cause to neighboring structures?
- Will a given vibrator be able to drive the pile to the required design depth? If so, at what speed? Are there soil types that strongly limit vibratory penetration depth?
- Are there ways to assess the vibratory capacity of a pile from the monitoring of its vibratory performance?
- Is there a vibratory testing technique and interpretation leading to estimating the long-term pile bearing capacity?

One can actually state that all issues will be properly tackled when combined into a comprehensive framework of analysis where proper understanding of soil behavior is the key. As clarified in Fig. 2, the present paper will focus on our current engineering ability to assess vibro-drivability, i.e. to predict the vibratory penetration log of a given pile into a given soil profile using a given vibrator. Testing undertaken to provide insight into the pile-soil-vibrator interaction and its modelling will be reviewed in Sections 4 and 5. We will then focus on some available methods to establish the vibratory performance of a pile from its vibratory capacity (Section 6), and look into the potential to establish the reverse relationship (Section 7). Finally, Section 8 provides suggestions for further research, design and practice.

Because of space limitations, the paper does not focus on other important engineering issues such as: bearing capacity of vibro-driven piles derived from soil characterization, vibrations transferred to the environment, and equipment specifications.

2 PILES AND VIBRATORY EQUIPMENT

2.1 *Vibrated Piles*

Pile types or profiles mostly used in combination with the vibratory driving technique include:

- sheet piles installed for temporary shoring, cofferdam and permanent retaining and containing walls,
- H-piles vibro-driven as deep foundations or vibrated to help install underground hydraulic barriers,
- Tubes to install cast-in-steel-shell (CISS) piles
- Precast prestressed concrete piles
- Steel profiles to vibro-compact granular soils at depth.

Port, harbor, near-shore and offshore projects very often take advantage of the vibratory penetration techniques, as the environment lends its self to substantial tolerance of vibratory disturbances.

Steel and concrete profiles are generally cylindrical or prismatic, and can be characterized by the following geometrical and mechanical properties :

A [m^2]: profile section
L [m]: profile length
χ [m]: profile perimeter
E [Mpa]: Material Young's Modulus
ρ [kg/m^3]: Material volumic mass

The profile section can be more fully characterized by its shape, and inside and outside perimeters if closed. This allows one to calculate the areas of the profile in longitudinal and transversal contact with the soil, once an embedment depth z [m] is assumed. The mass of the profile M_p equals ρAL [kg] while the longitudinal wave speed in the profile is given by $c=\sqrt{E/\rho}\ \ [m/s]$.

Although they may at time play an important role, transversal and flexural properties of the profile will generally be ignored in the analysis that confines itself to the longitudinal behavior of the profile.

2.2 *Mechanical action of a vibrator*

The mechanical action of a vibrator onto a profile consists of two part: a vibratory action and a stationary action.

The vibratory action imparted to the pile is produced by counter-rotating eccentric masses actuated within an "exciter block", as shown in Fig. 3a. The centrifugal forces acting as a result of inertial effects on an even number of symetrically moving masses

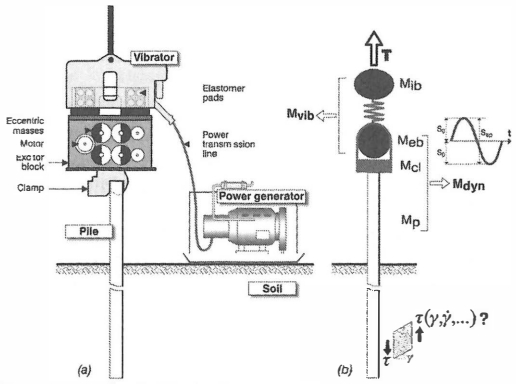

Figure 3. Mechanical action of a vibrator

combine into a sinusoidal vertical force :

$$F_v(t) = me.\omega^2 \sin(\omega t) = F_c \sin(\omega t) \qquad (1)$$

where
F_c = maximum centrifugal force of the vibrator [N]
me = eccentric moment of the vibrator [kg.m]
ω = angular frequency of the vibrator [rad/s]

Alternative quantifications of the angular frequency are the rotation speed R [rpm] and the frequency v [Hz], with :

$$R = 60\,v = 60 \cdot (\omega/2\pi) \qquad (2)$$

The vibratory action can be therefore assessed once both the eccentric moment and the operating frequency are known. That action will be balanced by reactive inertial effects of masses undergoing the imparted vibratory movement and by soil reactions opposing the profile movement. Provided the center of gravity of the rotating masses belongs at all times to the profile neutral axis, the exciter block is assumed to exert a purely longitudinal force onto the profile.

The exciter block is connected to the profile via a clamping device and is suspended to a carrier. The suspension device includes a vibration isolator mechanism consisting of a quasi-stationary heavy mass directly suspended to the suspension hook and an intervening spring, generally consisting of elastometer pads.

The vibrator can be viewed as a two degrees of freedom system moving in the longitudinal direction (see Fig. 3b) : an exciter block of mass M_{eb} and an isolator block of mass M_{ib}., sometimes called bias mass. Therefore $M_{vib} = M_{eb} + M_{ib}$. Those two masses are interconnected via an isolation spring with constant k_i. In addition to the effort generated by that spring, the mass M_{eb} is subjected to gravity (g) and the sinusoidal force described by eq. (1) whereas the mass M_{ib} is subjected to gravity and the suspension force T. The net quasi-stationary action on the pile resulting from the carrier operation and vibrator is the weight of the vibrator mass and its clamp M_{cl} deducted by the suspension force:

$$Fs\ [N] = (M_{vib} + M_{cl}) \cdot g - T \quad (3)$$

2.3 *Vibrator Movement*

The movement of the vibrated body will depend on its so-called dynamic mass and the soil resistance. Specifications of vibrators often list a "maximum amplitude" S_{sp}. That number [generally expressed in mm] corresponds to the *total* (i.e. double) amplitude of movement for a free hanging vibrator, thus assuming a dynamic mass consisting of the exciter block M_{eb} and the clamping device M_{cl}:

$$S_{sp} = 2\,s_0 = 2\,me/(M_{eb} + M_{cl}) \quad (4a)$$

It should be noted that the double amplitude does not depend on the operating frequency, as the center of mass of the free mechanical system remains stationary, irrespective of the frequency. The amplitude of the free hanging pile to be vibrated will always be smaller than the specified amplitude, as can be derived from eq. (4a), where the dynamic mass is increased by that of the pile (ρAL).

$$2s = S_{sp} \cdot \frac{M_{eb} + M_{cl}}{M_{eb} + M_{cl} + M_p} \quad (4b)$$

with s = actual (single) amplitude of the dynamic mass.

A power for the vibrator is often listed in the specifications. It generally corresponds to the nominal power of the motor actuating the eccentric masses. It does not correspond to standardized operational conditions of the vibrator in action. Power consumption is indeed dependent upon testing conditions. Barkan suggests that under pile vibratory conditions, the power follows a squared velocity law:

$$W\ [kW] = M_{dyn} \cdot n \cdot (s\,\omega)^2 = \beta_t \cdot W_t \quad (4c)$$

Experimental verification of that law shows the n value to depend on soil type and pile type; a range of 15 to 50 Hz is observed.

O'Neill and Vipulanandan (1989) provide an expression of the theoretical power required to maintain the vibrating regime of a dynamic mass in the absence of soil reaction but accounting for the presence of the isolating spring and the bias mass M_{ib}. That formula is however of limited practical use as it provides very low estimates of the power.

It is the author's opinion that power limitation of the equipment is neither sufficiently characterized, nor (therefore?) properly accounted for in vibratory driving analyses conducted to date.

2.4 *Types of vibrators*

Two main types of vibrators are commercially available: hydraulic and electrical. In both cases, the motor is housed in the vibrator and powered through a transmission line connected to a separate or carrier-mounted diesel-hydraulic or diesel-electric power pack (see Fig. 3a). Hydraulic vibrators are lighter than their electrical counterparts, because of the smaller size of the motor. The adjustment of the operating frequency is more readily available on the hydraulic vibrators, which also explain why they are more commonly used.

Five types of vibrators can be distinguished based on operating frequency and eccentric moments, as summarized in Table 1.

It can be noted that initial improvements of the vibratory driving technique targeted the speed of driving, whereas more recent improvements are attempting to mitigate environmental impacts associated with the technique. Noteworthy amongst recent developments is the "variable vibrator", which can adjust on-the-fly its effective eccentricity by shifting the phase angle between a multiple of 4 masses. The claimed advantage of such an adjustment is to avoid "soil resonance", a term coined after the observation that vibration levels pass through a peak upon vibration start-up and shut-down. This phenomenon will however be shown later not to be necessarily related to a particular frequency.

Vibrator choice amongst practicionners is generally based on experience and field verification. Rodger and Littlejohn (1980) have summarized that body of experience into a table recommending frequency and amplitude parameters for different piles and soil types. Those recommendations are reproduced herein as Table 2.

Table 1. Vibrator types

Type	Frequency range [rpm]	Eccentric moment [kg.m]	Maximum centrifugal force [kN]	Free hanging double amplitude [mm]
"Standard frequency"	1300-1800	up to 230	up to 4,600	up to 30
High frequency	2000-2500	6 to 45	400 to 2,700	13 to 22
Variable eccentricity	2300	10 to 54	600 to 3300	14 to 17
Excavator accessory	1800 to 3000	1 to 13	70 to 500	6 to 20
Resonant driver	6000	50	20,000 (in theory)	Self destructing

Table 2. Vibrators classification (after Rodger and Littlejohn, 1980)

Cohesive soils	Dense cohesionless soils		Loose cohesionless soils	
All cases	Low point resistance	High point resistance	Heavy piles	Light piles
High acceleration Low displacement amplitude	High acceleration	Low frequency. Large displacement amplitude		High acceleration
Predominant side resistance	Predominant side resistance.	Predominant end resistance.		Predominant side resistance.
Requires high acceleration for either shearing or thixotropic transformation	Requires high acceleration for fluidization	Requires high displacement amplitude and low frequency for maximum impact to permit elasto-plastic penetration		Requires high acceleration for fluidization
Recommended parameters				
ν > 40 Hz a: 6-20 g s : 1-10 mm	ν : 10-40 Hz a : 5-15 g s : 1-10 mm	ν : 4-16 Hz a: 3-14 g s : 9-20 mm		ν : 10-40 Hz a: 5-15 g s : 1-10 mm

3 SOIL BEHAVIOR UNDER VIBRATORY LOADING

3.1 *Fundamentals*

As the profile undergoes a vibratory vertical motion of amplitude s, it communicates to the lateral neighboring soil shear stresses and shear strains, as sketched in Fig. 3b. It is also forcing normal and po-tentially convective movement of soil below the pile toe.As those mechanisms govern soil resistance along the shaft and at the toe, the understanding of the shear stress/shear strain relationship, i.e. τ (γ), within the soil becomes of paramount importance.

That aspect of soil behavior has been more extensively studied within the field of earthquake engineering, leading to the characterization of so-called constitutive relationships, generally on the basis of laboratory testing of soil samples (mainly triaxial testing and simple shear testing). The constitutive relationships that represents the complex large-strain, dynamic and cyclic shear stress-strain strength, behavior of the medium surrounding the vibrating profile require the characterization of the following elements :

- Static stress-strain law expressing nonlinear behavior under monotonic loading and hysteresis upon strain reversal,
- Shear modulus at small strains and ultimate shear strength,
- Softening and increase of hysteretic damping with increasing strain,
- Effect of strain rate on initial shear modulus and ultimate strength,
- Degradation of properties resulting from the application of numerous cycles, and last but not least,
- Generation of excess pore pressure leading substantial loss of resistance and possibly to liquefaction.

The following paragraphs address key components of the constitutive relationships and provide insight on the intrinsic soil behavior in the vicinity of the vibrating profile.

3.2 *Static and Cyclic Stress-strain Behavior*

A typical soil response to uniform cyclic strains with amplitude γ_c is represented in Fig. 4, which highlights the following fundamental parameters:

G_{max} : initial (or tangent) shear modulus
τ_c : shear stress mobilized at γ_c
G_s: secant (or equivalent) shear modulus
λ : hysteretic (or intrinsic) damping ratio;

$$\lambda = \Delta W / 2\pi\gamma_c\tau_c \qquad (5)$$

with ΔW = Energy lost during a given cycle.

Both G_s and λ are strain-dependent parameters that need to be described by specific laws within a given cycle. τ_{max} is the ultimate shear strength, revealed at large strains. τ_{max} and G_{max} are shown to decrease with the number of cycles (cyclic degradation).

3.3 *Initial Shear modulus and ultimate shear strength (G_{max} and τ_{max})*

Numerous studies have dealt with the initial shear modulus to be used in earthquake engineering (e.g. Drnevich et al., 1967). Most of them are supported by parameters determined in the laboratory which are generally not available when a vibratory penetration issue arises. However, correlatins with CPT test results have been more recently developed (Seed and De Alba, 1986, Robertson and Wride, 1998)

3.4 *Secant Shear Modulus and Hysteretic Damping (G_s and λ)*

As can be observed in Fig. 4, G_s decreases with the shear strain during the initial monotonic loading. The curve that represents the initial monotonic loading is referred to as the initial "backbone" curve, because it also serves as the basis to generate the

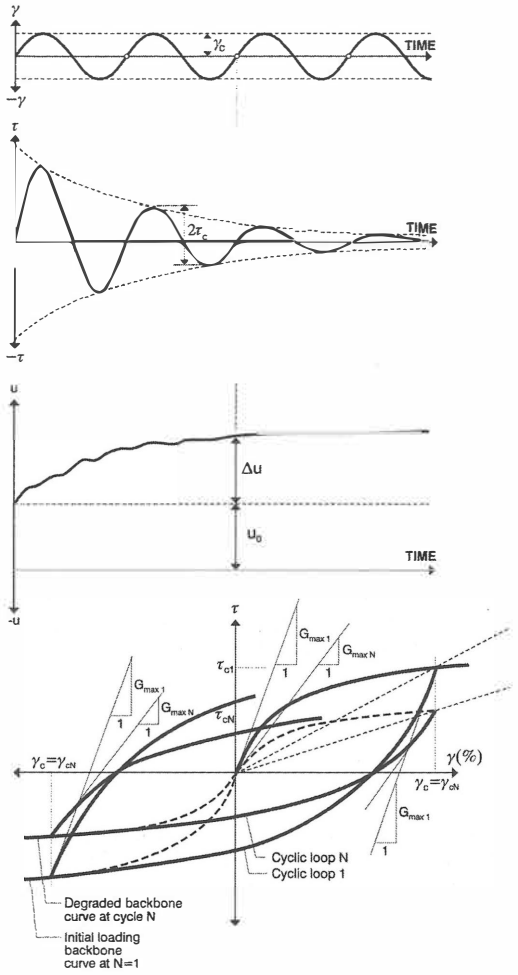

Figure 4. Soil Behavior under Constant Cyclic Shear Strain Amplitude Loading (From Vusetic, 1993; 1994)

family of curves corresponding to unloading and reloading. Kondner's mathematical formulation (1963) is frequently employed to describe the initial backbone curve in earthquake engineering. That hyperbolic law is best represented in terms of reduced variables, η, the mobilization ratio and δ, the relative shear :

$$\eta = \tau / \tau_{max} = \delta / (\delta + 1)$$

with $$\delta = \gamma / \gamma_r = \gamma \cdot G_{max} / \tau_{max} \qquad (6)$$

and $$\gamma_r = \tau_{max} / G_{max}$$

γ_r is called the reference strain. Two of the three parameters G_{max}, γ_r, and τ_{max}, are generally derived from laboratory experiments. More extensive laboratory surveys by Robertson and Wride (1998) point towards the upward curvature of the stress/strain curve at large cyclic strains.

From the point of maximum straining, the unloading curve is described by the following equation, in accordance with Masing's rules 1 and 2 (Masing, 1926):

$$\tau = \tau_0 (\gamma - \gamma_0) / (1/G_{max} + (\gamma - \gamma_0)/2\tau_{max}) \qquad (7)$$

The energy dissipated within a loop depends for a given soil on the amplitude of the cyclic strain. Empirical data collected in laboratory tests indicates that the damping ratio increases with γ_c as the soil undergoes higher plastic deformations.

Dobry and Vucetic (1987, Vucetic and Dobry, 1991, and Vucetic,1993 and 1994) have suggested a unifying approach to accommodate the influence of the nature of the material characterized by the plasticity index (PI), as indicated in Fig. 5

3.5 *Strain Rate Effects*

Although it is well known that undrained modulus and shear strength increase with increasing strain rate ($\dot{\gamma} = \partial\gamma / \partial t$), experimental data generated using different apparatuses and loading conditions lead to different conclusions. Viscosity mechanisms may well provide a suitable framework to understand the strain rate effect observed when comparing fast and slow undrained monotonic stress-strain curves, as well as to explain the roundness of the loop tips during a sinusoidal strain-controlled cyclic test. Evidence would point to the fact that sands and non plastic silts have very small viscosity in that their stress-strain loops exhibit sharp rather than rounded tips (Dobry and Vucetic, 1987).

The mathematical functions proposed in the literature to represent the nonlinear viscosity also depend on the type of experimental observations. A power law is often adopted :

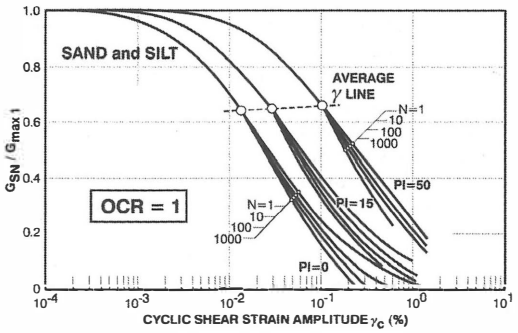

Figure 5. Soil stiffness degradation resulting from cyclic shear (Vucetic, 1993)

$$\tau_{kin} = \tau_{sta} \cdot \left(1 + J \cdot \dot{\gamma}^{n}\right) \quad (8)$$

with τ_{kin} = kinetic ultimate shear strength [kPa]
τ_{sta} = "static" ultimate shear strength [kPa]
$\dot{\gamma}$ = shear strain rate [s^{-1}]

The advantage of that mathematical form is that resistance does not vanish as the strain rate goes towards zero. The power law also requires the strain rate to vary by orders of magnitude to provide tangible increases in both the modulus and the ultimate strength. The J coefficient and n exponent depend on the nature of the soil. Based on pile driving data, n=0.2 and J=0.3 $s^{-0.2}$ have been suggested for plastic soils. J should therefore essentially depend on the plasticity of the soil and become quite limited for granular materials.

3.6 *Degradation Law*

When subjected to undrained cyclic loading involving a number N of large strain cycles, the soil structure continuously deteriorates, the pore pressure increases, and the secant shear modulus decreases with N. This process known as *cyclic stiffness degradation* can be best characterized on the basis of strain controlled tests for the type of loading involved with the vibratory penetration of piles. Typical results of strain-controlled tests are sketched in Fig. 5, where the degradation is clearly expressed by the decrease of the amplitude of the peak stress mobilized at successive cycles.

The quantification of the degradation process calls for the introduction of the degradation index Δ, defined by:

$$\tau_n = \Delta \cdot \tau_1 \quad (9)$$

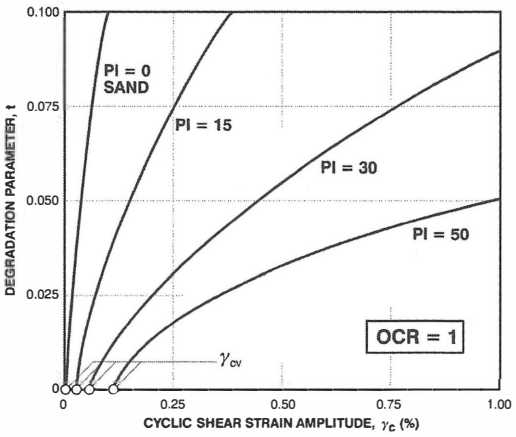

Figure 6. Effect of Plasticity Index (PI) on soil degradation (Vucetic, 1993)

Laboratory results conducted at constant cyclic strain show that in many soils, the degradation index after N cycles can be approximated by the following relationship as suggested by Idriss et al (1978):

$$\Delta = N^{-t} \quad (10)$$

The exponent t, called degradation parameter, depends mainly on the amplitude of the cyclic strain and the nature of the material (PI), as suggested by Dobry and Vucetic (1988) and as indicated in Fig. 6 Vucetic, 1993). It is noteworthy that the degradation parameter assumes a zero value at strains smaller than a cyclic "threshold" shear strain, γ_{cv} The threshold strain increases with the plasticity of the soil, as suggested in Fig. 6.

3.7 *Soil liquefaction*

Vibration induced compaction of saturated sands has received attention not only from the earthquake engineering community, but also from vibro-compaction specialists.

Recent advances tend to indicate that build up of pore pressures (eventually leading to liquefaction) and volume reduction of cyclically loaded materials are the expression of the same phenomenon, i.e. the irreversible tendency for a particulate arrangement to achieve a denser packing when sheared back and forth.

Under drained conditions, the volume reduction is immediate. Under undrained conditions, the tendency for volume reduction is expressed by an increase in the pore water pressure (see Fig. 7), such that the effective stress is reduced to a value that may be close to zero. It is then necessary to wait for the soil to consolidate in order to see the volume reduction take place.

The strain driven evaluation of the build up of pore pressure as suggested by Dobry et al. (1979) is an approach that lends itself to a direct transposition

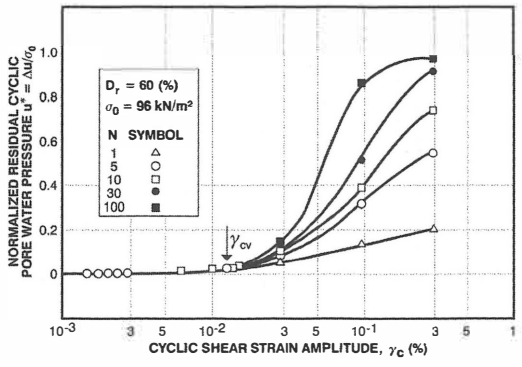

Figure 7. Build up of residual pore pressure in different sands in undrained cyclic strain-controlled tests (Dobry et al., 1982)

to the problem of the vibrations induced by a vertically vibrating pile. It also allows one to evaluate potential changes of the void ratio based on a cyclic strain rather than stress history, as supported by laboratory drained tests conducted on sands by Youd (1972). That framework of analysis entranced by the threshold cyclic strain concept embodies in a single model the intrinsic relationship between degradation and pore pressure build-up, with the advantage that it can be applied to general categories of soils (sands to clays)

The excess pore pressure generated during cyclic loading has been shown (see Fig. 7) to increase with the shear strain and the number of cycles for a given soil type. The damage parameter κ approach (Finn, 1981) can be adopted to evaluate the excess pore pressure δu resulting from a particular strain history, as characterized by the following equations :

$$du / d\sigma = \lambda / 4 \cdot \ln(1 + \kappa' 2) \qquad (11)$$

with Relative Energy Loss given by Eq. 5, and

$\kappa = \xi e^{\Sigma\gamma}$ (16) with $\Sigma = 5$ and

ξ = length of strain path
= $4 N \gamma_c$, for constant amplitude cycles (12)

4 PILE VIBRATORY DRIVING TESTING

The above discussion of soil behavior under cyclic loading does not encompass the particular geometry of the profile-soil interface, nor does it consider the continuous penetration of the profile that leads to successive exploration stages into "virgin" soil behavior. That is why a number of experiences have been conducted to reveal soil-structure interaction within a vibratory framework. Based on the ambition and complexity of the tested interface, one can categorize various experiences reported in the literature as conceptual, interface, and both reduced and full-scale testing.

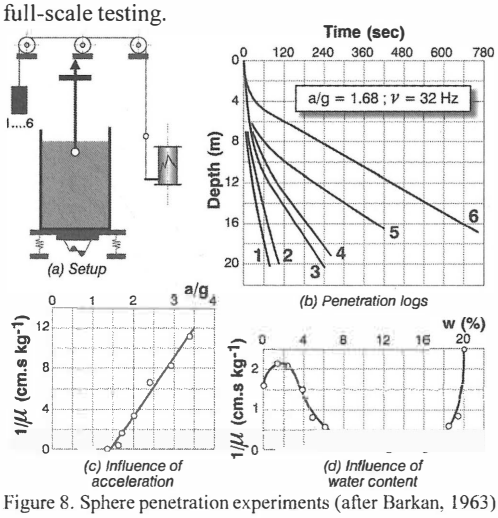

Figure 8. Sphere penetration experiments (after Barkan, 1963)

4.1 *Conceptual model testing*

Tests have been conducted by several Russian researchers to investigate the "vibro-viscous" resistance of soils. In particular, Barkan (1963) reports on the sphere test, shown in Fig. 8a, where a steel ball is sunk into a vibrated soil vessel with the assistance of a bias force. Penetration speed is shown to obey Stokes sedimentation law (see Fig. 8b), allowing one to determine an equivalent viscosity μ . The inverse of that equivalent kinematic viscosity [cm.s/kg] was shown to vary linearly with the relative level of acceleration (a/g), passed a threshold value of approximately 1.4 for a dry sand (see Fig. 8c). The influence of the water content on the "vibro-viscosity factor $1/\mu$" of a sand vibrated at constant a/g is also shown in Fig. 8d, highlighting the near total loss of vibro-penetrability at optimal water content.

4.2 *Pile-soil interface testing*

Soil shear strength resisting the pulling out of a vibrating steel plate against a normal stress controlled medium sand (vibratory direct shear box) has been investigated in the early days by Levchinsky and Savtchencko (Barkan, 1963). The friction coefficient ($\tan \phi = \tau/\sigma$) was shown to decrease with cyclic amplitude and frequency. The ultimate relative reduction of the friction was also shown to increase with the grain size within the investigated range shown in Fig. 9. Fig 9 shows that the sand vibratory friction angle can easily drop to ½ to 1/5 of its static value.

4.3 *Reduced scale tests*

Testing of model profiles in soil tanks were initially attempted by Bernhard (1968), Schmid and Hill (1966), continued by Rodger and Littlejohn (1980), Billet and Siffert (1985) and O'Neill et al (1990),

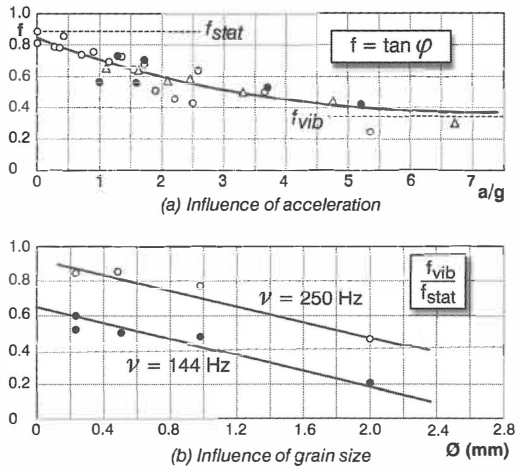

Figure 9. Vibratory friction of sand (after levehinsky and Savtchencko, as reported by Barkan, 1963)

and more recently by Viking (1998) and Holeyman et al (1999). The tests were generally conducted using a lightweight vibrator acting on a heavily instrumented profile. Monitoring included strain gauges, accelerometers and displacement transducers. The soil used was exclusively sand (dry, moist, or saturated), placed at a controlled density, and in some cases, confined at a controlled radial stress. Monitoring of the soil response involved accelerometers, total stress and pore pressure cells during installation as well as compaction and in situ testing after installation.

Insightful observations relative to the vibratory toe resistance have been reported by Schmid (1966), who identified three regimes, depending on the magnitude of the driving force :

- a sinusoidal resistance domain, for a driving force lower than the "resistance threshold"
- an impact domain, when the upward force exceeds the soil uplift resistance; the toe of the pile alternately separates from the soil and tamps it
- a phase instability domain, when the downward force exceeds the soil compressive resistance.

Rodger and Littlejohn (1980) call upon acceleration amplitude to distinguish:

- the elastic state ($a<0.6g$)
- the trans-threshold state ($0.6g<a<1.5g$), wherein most of the shear strength reduction takes place,
- the fluidized response state ($a>1.5g$).

Although their views are contradicted by some of Barkan's observations, these three different states are stated to be confirmed by dynamic direct shear tests performed by others.

Results of tank experiments have been reported in terms of friction reduction coefficients, potential optimal operation, and have shed some light on fundamental soil behavior. Correlations have been established between penetration speed and parameters induced by the vibrator (amplitude, frequency) and by the soil (grain size, relative density, and lateral stress). Although conclusions of the tests conducted under different conditions do not consistently agree, those experiments *generally* identified that:

- penetration speed increased when the relative density decreased and the bias mass increased
- friction was reduced to 30 to 50% of its static value, while a more limited reduction was noted for the toe resistance
- optimum operation of the hammer required at times that the frequency or eccentric moment be reduced, while energy transfer was of the order of 40% of the full theoretical power produced by the vibrator
- a number of observations cannot be explained.

Although reduced scale models are of use, they suffer from improper boundary conditions (at the tank limits) that significantly prevent the vibration energy from propagating away from its source.

4.4 *Full scale tests*

Because of inconsistencies in the conclusions derived from reduced scale tests, research has been conducted in several countries based on full-scale tests. Early full-scale programmes have been conducted by Barkan (1963) and Davisson (1970). Other programmes have been conducted by manufacturers on specific equipment, but lead to a limited diffusion of their conclusions. More recently, collective European programs have provided actual penetration speed, but within soil conditions that cannot be controlled, only characterized. Monitoring nowadays involvies acceleration, strain, pore pressure, penetration speed, making the tested profile a fully instrumented probe. Such programs have produced results that have not been fully analyzed or validated (BBRI, 1994, Sipdis, 1997, Viking, 2002); others are being presently conducted (IREX, 2000, Borel et al., 2002). Publication of such research results is usually appreciated by the profession.

5 PILE-SOIL-VIBRATOR INTERACTION MODELS

5.1 *Types of models*

Models that have been suggested by various authors differ in the way they account for mechanical engineering principles. We will review models purely based on (1) force equilibrium, (2) momentum conservation, (3) energy conservation, and (4) integration of the laws of motion.

5.2 *Force equilibrium models*

The force models aim at predicting whether a vibrator can or cannot overcome an estimated soil resistance. They will not provide an estimate of the driving speed. Jonker (1987) and Warrington (1989) have suggested, respectively:

$$F_C + F_I + F_S > \beta_0 . R_{so} + \beta_i . R_{si} + \beta_t \cdot R_t \qquad (13a)$$

$$F_v > \tau_s \cdot \chi \cdot z \qquad \text{provided } s > 2.38 \text{ mm} \qquad (13b)$$

With:

F_C = force generated by the vibrator, per eq. (1)
F_I = inertia forces of dynamic mass, = M_{dyn} . a
F_S = surcharge force, per eq. (3)
β_0 = empirical factor of shaft resistance outside pipe pile,
R_{S0} = soil resistance outside pile shaft,
β_i = empirical factor of shaft resistance inside pipe pile,
R_{si} = soil resistance inside pile shaft,
R_i = soil resistance at pile toe.

For sheet-piles Tunker Company recommends to replace $\chi . z$ [m^2] with 2.81 times the sheet-pile width.

5.3 *Energy based models*

Energy based models assume the following general form:

$$R.v_P = \beta_t . W_t + (F_i + F_s).v_P \quad (14a)$$

leading to a direct estimate of the penetration speed :

$$v_P = \beta_t \cdot W_t / (R - F_i - F_s) \quad (14b)$$

With:
R = soil resistance,
v_p = average rate of penetration in m/s,
W_t = theoretical power delivered to the system,
Fi = inertia forces of dynamic masses.

Davisson's formula (1970) to estimate the bearing capacity for the Bodine Resonant Driver suggests :

$$\beta_t = 1 - v \cdot s_e \cdot R/1000 \quad W_t \quad (15)$$

where s_e is an empirically determined set [mm/cycle] representing all energy losses.

Warrington (1989) has coined eq. (14b) as the 'Vibdrive' formula provided a value of 0.1 is used for β_t and the power W_t is calculated according to his procedure.

5.4 *Momentum conservation models*

Schmid (1968) has suggested a formula implying that, for steady-state penetration, the momentum of the total mass of the vibrator, additional bias mass (M_s), and pile accrued by gravity over a vibration cycle be balanced by the soil resistance impulse:

$$(M_s + M_{vib} + M_p) g \cdot T = \int_o^{T_c} R dt = \alpha R T_c \quad (16a)$$

with T_c = contact time between pile toe and soil within a cycle and α = coefficient between 0.5 and 1, generally assumed to be 2/3.

Conversely, the penetration speed follows a linear trend passed the threshold acceleration a_{min}, which becomes a key parameter to successfully apply the method and estimate T_c :

$$V_p = \frac{(a - a_{min})}{2v} \left[\frac{(M_s + M_{vib} + M_p) g}{R/\alpha} \right]^2 \quad (16b)$$

5.5 *Integration of laws of motion*

Comprehensive accounting of the laws of mechanics requires that movement be described at all times from inertial equilibrium conditions. The simplest models involve a single degree of freedom. 1-D models already offer more detailed description of some form of wave propagation, whereas 2-D models might provide future solutions that integrate all types of wave propagation (compression, shear, Rayleigh, etc..).

5.5.1 *Single degree of freedom (SDOF)*

Simplest models of the vibrator suggest that the dynamic mass be the focus of attention, thereby assuming that the pile behaves as a rigid body. Newton's second law can therefore be applied to the dynamic mass :

$$a = \frac{me \cdot \omega^2 \sin(\omega t)}{M_{dyn}} \quad (17a)$$

where

$$M_{dyn} = M_{eb} + M_{cl} + M_p \quad (17b)$$

Holeyman (1993) has suggested a method that integrates the inertial effects of the excess force. That excess force is defined as the difference between the sinusoidal driving force and the opposing soil resistance. A distinction is made between the skin friction, which is reversible (Uplift resistance = Downward resistance) and the toe resistance, which cannot produce uplift resistance. Attention is also paid to the clutch resistance, which is combined with the skin friction.

The soil degraded resistance at the toe and along the shaft is estimated from CPT test results where the friction ratio and acceleration ratio are used to assess the severity of degradation. The method involves an iterative procedure to identify the coexisting acceleration and soil resistance (17b). The driving speed is obtained by intuitively integrating the net downward and upward accelerations over a complete cycle. The method have been verified and liquefaction parameters further refined through calibration with full-scale tests (BBRI, 1994)

Gonin (1998) has followed a similar approach that analytically integrates the effects of an excess force, as shown in Fig. 10. The integration is however performed soleby on the toe resistance, while the skin friction influence is accounted for in terms of damping of the driving force. In addition, the wave equation theory is used to estimate the displacement accrued at the toe over the period of net force exceedance.

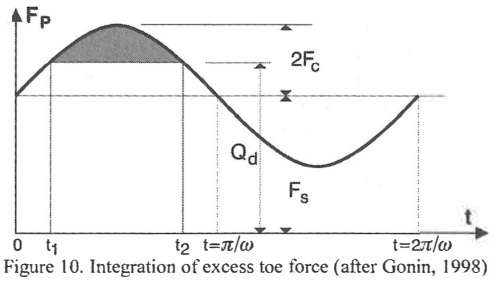

Figure 10. Integration of excess toe force (after Gonin, 1998)

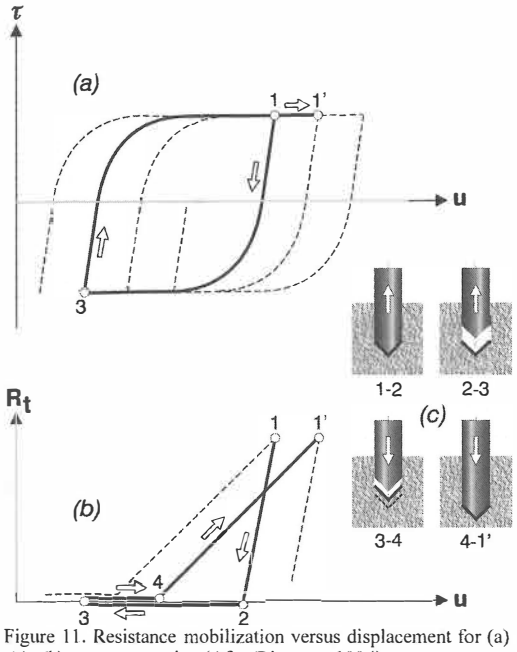

Figure 11. Resistance mobilization versus displacement for (a) skin (b) toe compression (After Dierssen, 1994)

Dierssen (1994) has used a numerical integration scheme to closely follow the time dependence of the skin and toe resistances. Figure 11 provides the shape of the resistance mobilization versus displacement for both skin and toe resistance. One can note that separation of the pile from the soil at the toe is explicitely accounted for.

5.5.2 *Radial 1-D model*

Holeyman (1993b) have suggested the use of a radial discrete model to calculate the vertical shear waves propagating away from the pile. The model, shown in Fig. 12, consists in a succession of concentric cylinders with a linearly increasing depth. The equations of movement are integrated for each cylinder based on their dynamic shear equilibrium in the vertical direction, in a manner similar to that used by Smith (1960) in the longitudinal direction.

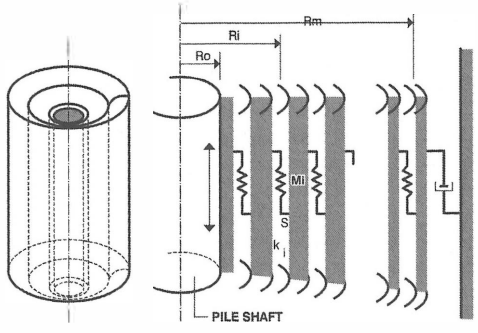

Figure 12. Radial 1-D model (Holeyman, 1993b)

The model allows the constitutive relationships described in Section 3 to be readily deployed. The major advantage of that shear wave propagation model is to closely follow the development of degradation as more cycles are simulated. It can also provide insight into vibration levels in the vicinity of the pile. Both features are illustrated by Fig. 13 which provides the effective particle velocity calculated at several distances away from a profile upon vibrator start up. An apparent resonance is indicated, whereas the model does not include a longitudinal or radial dimension that could explain the frequency at which the peak vibration is noted : why? Simply because the model most probably reproduces two soil-pile interaction vibratory modes: the coupled mode and the uncoupled mode.

In the coupled mode (similar to Schmid's sinusoidal domain), the soil remains in contact with the slowly vibrating profile, and the transfer of energy from the pile to the soil is nearly perfect. As the vibrator linearly accelerates (between 0 and 0.5 seconds), vibration levels tend to increase with the square of time since start up. However, as the soil begins to degrade, its shear modulus decreases and the specific shear impedance reduces, leading to loss in the energy transfer. At that point, the coupling between soil and pile suffers some slippage, and therefore time lag. After a sufficient number of cycles, the soil has significantly degraded, and has (60 seconds ageing skipped in Fig. 13) entered into li-quefaction.

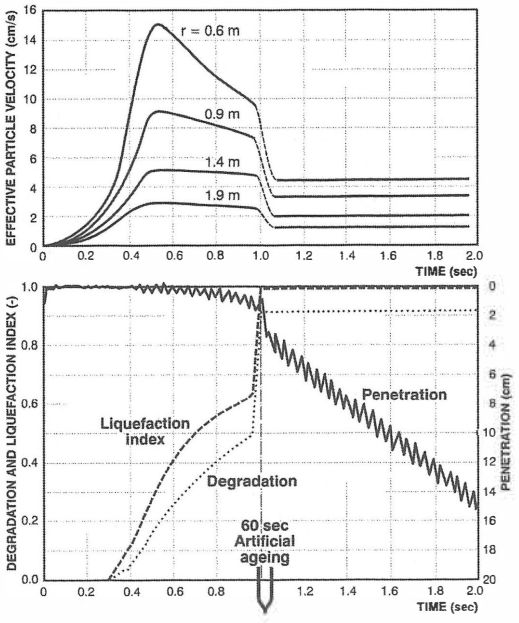

Figure 13. Vibration levels and penetration state parameters estimated upon vibrator startup and regime

At the shear modulus of the soil in contact with the profile is nearly zero, and very little energy can pass through the fluidized surrounding zone. The soil in the vicinity of the profile cannot anymore follow the profile movement, from which it uncouples itsel, resulting in a lower level of vibration. That example demonstrates that apparent resonance of soil vibration may be no more than the transient combination of increased rotation speed and soil degradation. The model can also shed light on "damping" as it clearly separates geometric damping from the energy losses attributable to viscous and hysteretic behavior.

A refinement to the above described 1-D radial model was developed by Vanden Berghe and Holeyman (2002). The so-called VIPERE model (for VIbratory PEnetration Resistance), actually implements hypoplastic constitutive behaviour into the geometric model suggested by Holeyman (1994). The soil behaviour is assumed to be hypoplastic and modeled using the Bauer (1996) and Gudehus (1996) constitutive law. More details are provided in Vanden Berghe and Holeyman (2002). One rare feature of the model is its ability to follow pore pressure variations through the various states experienced by the soil during the cycles as a result of dilatant or contractive behaviour of the soil skeleton. Typical simulations for a pile driving problem are presented in Fig. 14 and 15, which emphasize that the three-dimensional character of the volume change trends can be accomodated respectively in a pure shear for the skin friction along the shaft as well as in compression under the pile toe.

5.5.3 *Longitudinal 1-D models*

Few authors have adapted Smith's (1960) classic lumped parameters model to represent the longitudinal behavior of a pile subjected to vibratory driving. Gardner (1981) and Chua et al. (1981) have developed a wave-equation computer code where the vibrator is represented by a two-mass system, separated by a soft spring, while the exitor black is subjected to a sinusoïdal force (cfr. eq. (1)); as shown in Fig. 14. The soil behavior is represented by spring-slider-dasplot systems, according to Smith's early suggestion.

Middendorp and Jonker (1988), as well as Ligterink et al. (1990) used the TNOWAVE computer program to analyze the driveability of offshore vibratory driven pipe piles, based on the methods of characteristics. The authors identify the need for a soil model able to describe the degradation of the soil resistance as a function of the oscillation history, and warn that soil parameters may depend on opera- ting frequency and pile movement amplitude.

Moulai-Khatir et al. (1994) have developed together with the University of Houston, the so-called VPDA computer program (for Vibratory Pile Driving Analysis) wherein the action of the hammer is replaced by a static surcharge load and a sinusoïdal load. The soil model was modified from Smith's original in that hyperbolic mobilization curves were adapted for the shaft and toe resistance, as shown in Fig. 17. A simple viscous damper was used to model damping along the shaft, while no damping was deemed necessary at the pile toe.

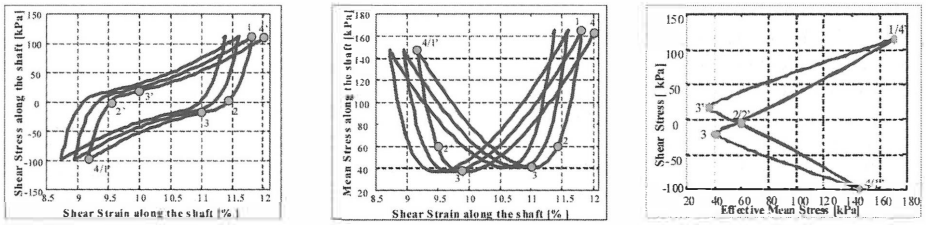

(a) (b) (c)

Fig. 14: Soil resistance along the pile shaft during vibratory driving: (a) hysteresis loops, (b) mean stress evolution and (c) vertical shear stress vs effective radial normal stress

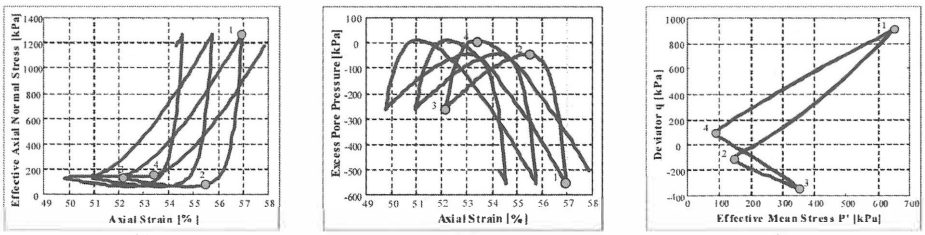

(a) (b) (c)

Fig. 15: Soil resistance at the pile base during vibratory driving: (a) evolution of the effective normal axial stress, (b) evolution of the pore pressure, (c) stress path.

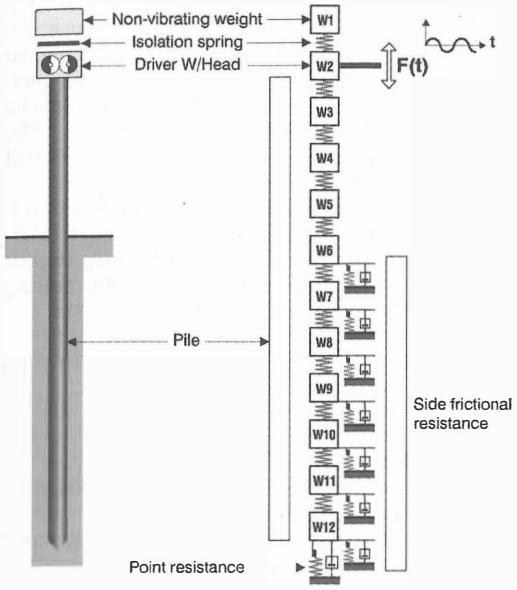

Figure 16. Longitudinal 1-D model

It should also be noted that the GRLWEAP program has included in its latest versions (GRL, 1998) the capacibilty to model vibratory hammers.

6 VIBRO-DRIVABILITY ANALYSIS

Most of the models discussed in the previous sections should be able to provide a reasonnable match of calculations with relevant field observations provided the models parameters are properly calibrated.

The use of energy balance methods is discouraged by the author, while force equilibrium methods are of limited use because they do not provide vibratory penetration speed. Momentum based methods may produce a penetration speed very similar to that obtained through integration of the laws of notion of a rigid body. Finally, wave equations methods should not produce penetration speeds significantly different form those obtained form a rigid body analysis, provided the vibrator speed is lower than the resonant frequency of the pile, which is generally the case.

Exceptions to that general case include the Bodine Resonant driver and very long piles for offshore applications (L>50 m).

In the author's opinion, the most critical parameter to assess in order to produce a resonable prediction of vibro-drivability is the soil resistance to vibratory driving.

That is unfortunately where pertinent information and recent consistent experimental data is cruelly missing. The reliability of the predicted vibro-penetration log will strongly depend on the degradation parameters adopted to assess the vibratory penetration resistance form the soil investigation results. The author's experience leads him to use the following crude ultimate degradations coefficients : 0.15 in sand, 0.4 in silt, and 0.65 in clay for skin friction; as well as 0.55 in sand, 0.7 in silt and 0.85 for end bearing.

A more involved assessment of the degradation coefficient has been suggested (Holeyman, 1996) based on CPT test results. In that method, the soil driving resistance is obtained by interpolation between a static value and an ultimately degraded value. The static base (q_s) and shaft (τ_s) resistance profiles derived from Cone Penetration (CPT) tests results, i.e. from the cone resistance q_c and local unit skin friction f_s (E1 cone).

The ultimately liquefied base (q_l) and shaft (τ_l) unit soil resistances are derived based on an exponential law as expressed below :

$$q_l = q_s \left[(1 - 1/\Lambda) \cdot e^{-1/FR} + 1/\Lambda \right] \quad (18a)$$

$$\tau_l = \tau_s \left[(1 - 1/\Lambda) \cdot e^{-1/FR} + 1/\Lambda \right] \quad (18b)$$

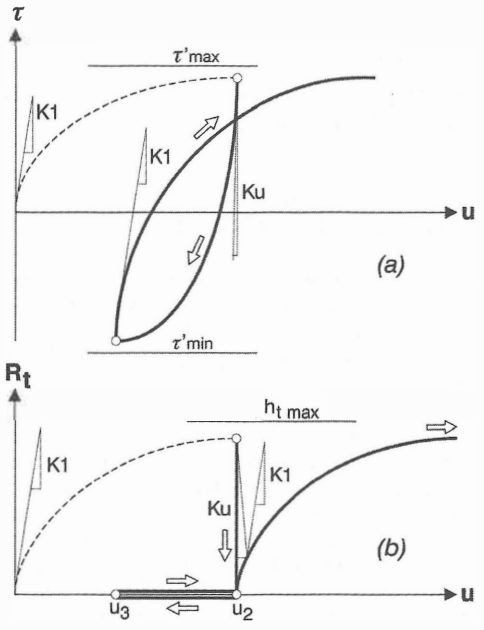

Figure 17. Resistance mobilization for (a) skin friction (b) toe compression (After Moulai – Khatir et al., 1994)

where
q_l = liquefied soil base resistance [kPa]
τ_l = liquefied soil shaft resistance [kPa]
FR = friction ratio as measured in a CPT test with El cone (percentage of the mantle friction to the cone resistance, i.e. FR = 100 f_s / q_c)
Λ = empirical liquefaction factor expressing the loss of resistance attribuable to liquefaction (Λ will be higher for saturated and loose sands and is chosen in the range of 4 to 10)

The driving base (q_d) and shaft (τ_d) unit resistances are derived from the static and the "liquefied" soil resistance depending on the vibration amplitude following an exponential law as expressed below :

$$q_d = (q_s - q_l)e^{-\alpha} + q_l \tag{19a}$$

$$\tau_d = (\tau_s - \tau_l)e^{-\alpha} + \tau_l \tag{19b}$$

where
q_d = driving base unit resistance
τ_d = driving shaft unit resistance
α = acceleration ratio (= a/g) of the pile, as obtained from Eq. (17a)

At each depth z the vibratory pile driving resistance is calculated :

$$R_{base} = q_d \cdot \Omega \tag{20a}$$

$$R_{shaft} = \chi \cdot \int_{z=0}^{z=D} \tau_d \cdot dz \tag{20b}$$

where Ω is the pile section, χ the pile perimeter and D the pile penetration.

7 BEARING CAPACITY FROM INSTALLATION MONITORING

Because soil resistance degradation is significant during vibratory driving, one should expect it a challenge to estimate the static bearing capacity from the end of penetration vibratory performance of a driven profile.

In the impact driving practice, it is recognized that end of driving (EOD) data generally provides a safe estimate of the pile capacity; that is why beginning of restrike (BOR) or "retap" data is strongly advised to the owner who wishes to tap the value of letting the soil set up. If the end of Vibratory driving (EOV) data is used, methods to estimate the static capacity should allow for recovery of soil degradation, as highlighted in Fig. 2. However significant uncertainty should be expected in the process because the inverse of observed degradation coefficients may range between 2 and 10

That is why extreme caution is warranted when applying so-called pile Vibratory driving (PVD), formulae, even more so than already much detracted (impact) pile driving formulae. A limited number of such PVD formulae have been published; however only one has been, to the author's knowledge been extensively field tested. The "Snipe" formula is therefore the only one that will be discussed in this paper.

The formula is a field-based method was developed in the former Soviet Union according to Steffanof and Boshinov (1977). The following empirical formula is used to predict the static bearing capacity Q_u :

$$Q_u = \frac{1}{\beta}\left(\frac{25.5 \cdot W}{\nu \cdot s} + F_t\right) \tag{21}$$

where
Q_u = load capacity, in [kN];
W = power used by the vibrator to drive the pile, in [kW]
F_t = total weight (force) of vibro-hammer and pile, in [kN]; = $(M_{vib} + M_p)g$
$1/\beta$ = empirical loss coefficient (in Soviet practice $1/\beta$ is safety taken to be 5 in cohesionless soils) reflecting the influence of driving on soil properties.

The bearing capacity in of vibro-driven pipe piles has been verified by PDA monitoring the behavior of the finished product at the beginning of impact restrike. This of course requires that a specific BOR procedure be enforced a sufficient time after the EOV installation, in order to allow pore pressures to dissipate and accrue soil setup.

The monitoring of the installation of vibratory driven piles is not at all as widely spread as for impact driven piles. Recent improvements in the field monitoring devices (PDA, TNO-System, etc) now allows the geotechnical engineer to control pile acceleration, stress and energy. However, there is no equivalent interpretation of the data to the CASE formula or CAPWAP method, available for nearly 15 years in the impact driven products.

Field monitoring provides a tremendous advantage in controlling the effective performance of the vibratory hammer, as illustrated by the following case history reported by Holeyman et al. (1996).

That case involved the installation of a 20.6 m long tubular steel pile with a thickness of 9.5 mm and a diameter of 1 m on a site in Kortrijk (B). Figure 18 shows the subsoil profile as depicted by a CPT test (cone M4) performed at the site. The water table was encountered at a depth of –1.8 m. The upper twelve meters consist of very soft river deposits; below the underlying sandy layer was found a very stiff tertiary clay layer in which the tube had to be driven.

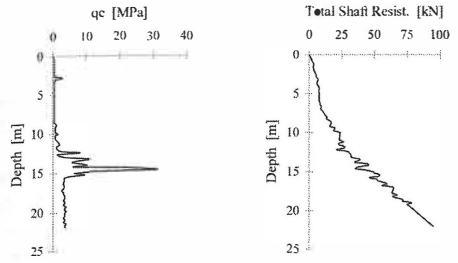

Figure 18. Subsoil profile site at Kortrijk

A preliminary calculation using eqs. (17) through (20) pointed out that the necessary time to install the pile to a depth of 20 m with a PTC

30HFV vibratory hammer was 13½ minutes. However, driving met refusal at a depth of 11 m.

The reason for the difficult driving and the difference between the predicted and the observed penetration speed was explained by measurements taken during the actual driving of the pile. The pile vibration amplitude was measured by means of a velocity transducer placed at the pile head and a velocity transducer (protected by a cover) at the pile toe.

Figure 19 shows the monitored amplitude of vibration at the pile top and at the pile base upon loss of drivability. The observed frequency was 38 Hz.

From the measurement results, one can observe that :

- the vibration amplitude at the pile top (0.65 mm zero to peak) is considerably less than the nominal vibration amplitude which is,

$$\frac{me}{M} = \frac{me}{M_{vibr} + M} = \frac{26000 kg.mm}{(6500 + 4820) kg} = 2.3 mm$$

- the amplitude at the pile base (0.45 mm zero to peak) is smaller than the amplitude at the pile top (0.65 mm)

It would appear that the pile base amplitude (0.45 mm) is not sufficient to allow the pile to penetrate as the stress-strain behaviour for clayey soils is primarily elastic for small amplitudes. Possible explanations for that observation were considered :

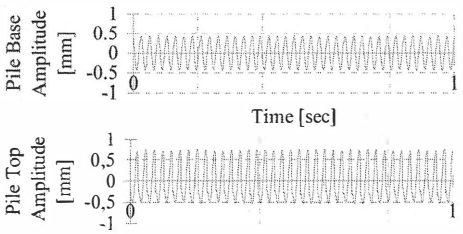

Figure 19. Record from the vibration amplitude upon refusal

- An important soil (i.e. clay) mass was sticking to the vibrating pile, leading to a more important vibrating mass, leading to a smaller vibration amplitude.
- The vibratory hammer was unable to deliver the required energy, and thus maintain its nominal amplitude or frequency. A characteristic of the PTC variable eccentric hammers is that a lack of power results in a reduction of vibration amplitude (rather than a reduction of frequency (Houzé, 1994)).
- A smaller amplitude at the pile base was obtained due to the elasticity of the pile.

By applying the observed vibration amplitude to the calculation model (Figure 20), a much better correlation between the calculated and the observed penetration time was obtained. The pile was placed at the bottom of an excavation at –2.5 m and penetrated 4.5m under its own weight. As a result, observed and calculated penetration rates are reported starting at level - 7 m. Figure 20 evidences that the difference for the predicted and observed penetration times for the site in Kortrijk was not due to an incorrect estimation of the dynamic soil resistance but due to an incorrect estimation of the vibration amplitude, which happened to be limited by the nominal power of the power pack. A more powerful power pack was brought on site and the piles could be vibrated to design depth using the same vibrator.

8 SUGGESTIONS FOR FURTHER RESEARCH, DESIGN, AND PRACTICE

After reviewing the present state-of-the-art of vibratory driving, the following suggestions for further consideration are offered :

- soil mechanics research is needed in the area of large cyclic deformation to better understand and assess the effects of degradation and liquefaction under those extreme conditions,

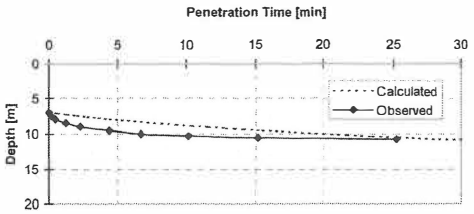

Figure 20. Predicted and Observed penetration log at Kortrijk site compared with predicted log using actual vibratory amplitude

- full scale vibratory driving tests, with extensive field monitoring, will be required preferably to reduced scale laboratory tests, which suffer from improper energy dissipation boundary conditions,
- potential and transferred power of vibrators need to be better defined, as well as modeled for better description of the mechanical behavior of vibrators,
- peak vibration of the soil surrounding a profile upon vibrator start up does not necessarily imply soil resonance; it can also result from the combination of increasing frequency and degrading soil resistance,
- monitoring of vibrated profiles is recommended with the view to emulate the benefits accrued by a similar practice for driven profiles, and
- procedures for vibratory loading tests should be developped.

9 REFERENCES

Bauer, E. (1996). "Calibration of a Comprehensive Hypoplastic Model for Granular Materials." Soils and Foundations, Vol. 36, N°1, pp.13-26.

Barkan, D.D., (1963), Méthodes de vibration dans la construction, Dunod, Paris, 302 p. *(French translation of Original in Russian "* Vibrometod V Stroïteljstve, 1960)

BBRI .(1994). High performance vibratory pile drivers base on novel electromagnetic actuation systems and improved understanding of soil dynamics, *Progress reports of the BRITE/EURAM research contract CT91-0561*, 1994.

Bernhard, R.K., (1967), Fluidization phenomena in soils during vibro-compaction and vibro-pile-driving and –pulling. Hanover, NH 1967, 58 pp., *US Army Cold Regions Research and Engineering.*

Billet, P., Siffert, J.G., (1989). "Soil-sheet pile interaction in vibro-piling" *Journal of Geotechnical Engineering, ASCE*, Vol. 115, N° 8, pp. 1085-1101

Borel, S. et al. (2002), "Full-scale behaviour of vibratory driven piles in Montoir", Proceedings of Transvib2002 Conference, Louvain-la-Neuve, Sept 9-10, 17 p.

Chua, K.M., Gardner, S., Lowery, L.L., (1987). "Wave Equation Analysis of a Vibratory Hammer-Driven Pile", *Proc. Offshore Technology Conf.*, Vol. 4, pp. 339-345

Davisson, M.T., (1970). "BRD Vibratory driving formula", *Foundation facts*, Vol. 1, N° 1, pp. 9-11

Dierssen, Guillermo, (1994), "Ein Bodenmechanisches Modell zur Beschreibung des Vibrationsrammens in körningen Böden", *Doctoral Thesis,* University of Karlsruhe, Germany

Dobry, R., Ladd, R.S., Yokel, F.Y., Chung, R.M. and Powell, D. (1982). "Prediction of Pore Water Pressure Buildup and Liquefaction of Sands During Earthquakes by the Cyclic Strain Method". *National Bureau of Standards Building Science Series 138,* July 1982, 150 pp.

Dobry, R. and Swiger, W.F. (1979). "Threshold Strain and Cyclic Behavior of Cohesionless Soils". *Proc. 3rd ASCE/EMDE Specialty Conference.* Austin, Texas, pp. 521-525;

Dobry, R. and Vucetic, M. (1987). "State-of-the-Art Report: Dynamic Properties and Response of Soft Clay Deposits". *Proceedings of the Intl. Symposium on Geotechnical Eng. of Soft Soils,* Mexico City, Vol. 2, pp. 51-87.

Drnevich, V.P., Hall, J.R., Jr., and Richart, F.E., Jr. (1967). "Effects of Amplitude of Vibration on the Shear Modulus of Sand." *Proceedings of the International Symposium on Wave Propagation and Dynamic Properties of Earth Materials,* Albuquerque, N.M., pp. 189-199.

Finn, W. D. L. (1981) "Liquefaction Potential: Developments Since 1976", *Proceedings, Intl. Conf. on Recent Advances in Geotechnical Earthquake Engineering and soil Dynamics, St.* Louis, Missouri, Vol. II, pp. 655-681.

Gardner, Sherrill, (1987). "Analysis of vibratory driven pile". *Proc. of 2nd Int. Conf. on Deep Foundation,* Luxembourg, 5-7 May, pp. 29-56.

Gonin, J. (1998), Quelques réflexions sur le vibrofonçage, *Revue Française de Géotechnique,* N° 83, 2ème trimestre, pp. 35-39

Gudehus, G. (1996). "A comprehensive constitutive equation for granular materials. " Soils and Foundations, Vol. 36, N° 1, 1-12.

Hardin, B.O. and Black, W.L. (1968). "Vibration Modulus of Normally Consolidated Clay." *Journal of the Soil Mechanics and Foundations Division,* ASCE, Vol. 94, No. SM2, Proc. Paper 5833, pp. 353-369.

Holeyman, A. (1985) "Dynamic non-linear skin friction of piles," *Proceedings of the International Symposium on Penetrability and Drivability of Piles*, San Francisco, 10 August 1985, Vol. 1, pp. 173-176.

Holeyman, A. (1988) "Modeling of Pile Dynamic Behavior at the Pile Base during Driving," *Proceedings of the 3rd International Conference on the Application of Stress-Wave Theory to Piles*, Ottawa, May 1988, pp. 174-185.

Holeyman, A. (1993a) "HYPERVIB1, An analytical model-based computer program to evaluate the penetration speed of vibratory driven sheet Piles", Research report prepared for BBRI, June, 23p.

Holeyman, A. (1993b) "HYPERVIBIIa, An detailed numerical model proposed for Future Computer Implementation to evaluate the penetration speed of vibratory driven sheet Piles", Research report prepared for BBRI, September, 54p.

Holeyman, A. & Legrand, C. (1994). Soil Modelling for pile vibratory driving, International Conference on Design and Construction of Deep Foundations, Vol. 2, pp 1165-1178, Orlando, U.S.A., 1994.

Holeyman, A., Legrand, C., and Van Rompaey, D., (1996). A Method to predict the driveability of vibratory driven piles, *Proceedings of the 3rd International Conference on the Application of Stress-Wave Theory to Piles*, pp 1101-1112, Orlando, U.S.A., 1996.

Houzé, C. (1994). HFV Amplitude control vibratory hammers : piling efficiency without the vibration inconvenience, in DFI 94, pp. 2.4.1 to 2.4.10, *Proceedings of the Fifth International Conference and Exhibition on Piling*

and Deep Foundations, Bruges, Belgium, 1994.

Idriss, I.M., Dobry, R, and Singh. R.D. (1978). "Nonlinear Behavior of Soft Clays during Cyclic Loading." *J. Geotechnical Engineering Div.*, ASCE, 104(GT12), pp. 1427-1447.

IREX (1998), Vibrofonçage des pieux et palplanches – Etude exploratoire, (by Le Tirant, P., Borel, S., Gonin, H., Guillaume, D. and Longueval, A.)

Jonker, G., (1987). "Vibratory Pile Driving Hammers for Oil Installation and Soil Improvement Projects". *Proc. of Nineteenth Annual Offshore Technology Conf.*, Dallas, Texas, OTC 5422, pp. 549-560.

Kondner, R. L., (1963). "Hyperbolic Stress-Strain Response: Cohesive Soils." *Journal of the Soil Mechanics and Foundations Division*, ASCE, Vol. 89, No. SM1, pp. 115-143, Jan.

Ligterink, A., van Zandwijk, C., Middentorp, P., (1990). "Accurate vertical pile installation by using a hydraulic vibratory hammer on the Arboath project". *Proc. 22nd annual Technology Conf. in Houston*, Texas, May 7-10, pp. 315-326.

Masing, G. (1926), "Eigenspannungen und Verfeistigung beim Messing", *Proceedings of Second International Congress of Applied Mechanics*, pp. 332-335.

Midendorp, P. and Jonker, G. (1988), Prediction of Vibratory Hammer Performance by Stress wave Analysis, *Preprint to the 3rd Int. Conf. on the Application of Stresswavre Theory to Piles*, Ottawa

Moulai-Khatir, Reda. O'Neill, Michael W., Vipulanandan, C., (1994). "Program VPDA Wave Equation Analysis for Vibratory Driving of Piles", *Report to The U.S.A. Army Corps of Engineers Waterways Experiments Station. Dept. of Civil and Environmental Engineering*, UHCE 94-1, Univ. of Houston, Texas, August 1994, 187 pp.

Novak, M., Nogami, T., and Aboul-Ella, F. (1978). "Dynamic Soil Reactions for Plane Strain Case", *J. Engrg. Mech. Div.*, ASCE, 104(4), 953-959.

NRC (1985). "Liquefaction of Soils During Earthquakes." National Research Council Committee on Earthquake Engineering, Report No. CETS-EE-001, Washington, D.C.

O'Neill Michael W., Vipulanandan, C., (1989). "Laboratory evaluation of piles installed with vibratory drivers". *National Cooperative Highway Research Program*, Report n° 316, National Research Council, Washington, DC. Vol. 1 pp. 1-51. ISBN 0-309-04613-0

O'Neill Michael W., Vipulanandan, C., Wong, D., (1990). "Laboratory modelling of vibro-driven piles". *Journal of Geotechnical Engineering, ASCE*, Vol. 116, N° 8, pp. 1190-1209

Robertson, P.K. and Wride, C.E. (1998). "Evaluating cyclic liquefaction potential using the cone penetration test", Canadian Geotechnical Journal, No. 35, pp. 442-459.

Rodger, A.A. and Littlejohn, G.S. (1980). "A study of vibratory driving in granular soils". *Geotechnique*, Vol. 30, n° 3, pp. 269-293.

Seed, H.B. and Idriss, I.M. (1970). "Soil Moduli and Damping Factors for Dynamic Response Analyses." Earthquake Engineering Research Center, College of Engineering, University of California, Berkeley, Report No. EERC 70-10.

Seed, H.B. and De Alba, P. (1986) "Use of SPT and CPT Tests for Evaluating the Liquefaction Resistance of Sands" *Proc. INSITU 86*, VA, 22 p.

Schmid, W.E., (1969). "Driving resistance and bearing capacity of vibrodriven model piles". *American Society of Testing and Materials Special Techn.*, Publ. 444, pp. 362-375

Schmid, W.E. & Hill, H.T. (1967). "A rational dynamic equation for vibro driven piles in sand". *Symp. Dynamic Properties of Earth Materials. New Mexico University*, p. 349.

Smith E.A.L., (1960). "Pile-driving analysis by the wave equation". *Journal of the Soil Mechanics and Foundations Divisions, ASCE*. Vol. 86, August 1960.

Vanden Berghe, J-F, (2001) "Sand Strength degradation within the framework of pile vibratory driving", doctoral thesis, Université catholique de Louvain, Belgium, 360pages.

Viking, K., (1997). "Vibratory driven pile and sheet piles – a literature survey", *Report 3035, Div. of Soil and Rock Mechanics, Royal Institute of Technology*, Sweden, 75 p.

Viking, K., (2002). "Vibratory driveability –a field study of vibratory driven sheet piles in non-cohesive soils" *PhD thesis 1002, Div. of Soil and Rock Mechanics, Royal Institute Technology*, Stockholm, Sweden, 281 pp, ISSN 1650-9501.

Vucetic, M. and Dobry, R. (1988). "Degradation of Marine Clays Under Cyclic Loading. *ASCE Journal of Geotechnical Engineering*,Vol. 114, No.2,pp.133-149.

Vucetic, M. and Dobry, R. (1991). "Effect of Soil Plasticity on Cyclic Response." *ASCE Journal of Geotechnical Engineering, Vol.* 117, No. 1, pp. 89- 107.

Vucetic, M. (1993). "Cyclic Threshold Shear Strains of Sands and Clays", Research Report, UCLA Dept. of Civil Engineering, May 1993.

Vucetic, M. (1994). "Cyclic Threshold Shear Strains of Sands and Clays", Paper in print, *ASCE Journal of Geotechnical Engineering*

Warrington, Don. C., (1989). "Driveability of Piles by vibration". *Deep Foundations Institute 14th Annual members Conf.*, Baltimore, Maryland, USA, pp. 139-154.

Westerberg, E., Massarch, K. Rainer. Eriksson, K., (1995). "Soil resistance during vibratory pile driving", *Proc. to Int. Symposium on Cone Penetration Testing*, Linköping, Sweden, Vol. 3, Report 3.41, pp. 241-250.

Youd, L.T. (1972). Compaction of sands by repeated shear straining, *Journal of the Soil Mechanics and Foundations Division*, 1972, Proc. ASCE, Vol. 98, SM7, pp. 709-725.